

Multiple Opposing Constraints Govern Chromosome Interactions during Meiosis

Doris Y. Lui^{1,2a}, Cori K. Cahoon^{1,2b}, Sean M. Burgess^{1*}

Department of Molecular and Cellular Biology, University of California Davis, Davis, California, United States of America

Abstract

Homolog pairing and crossing over during meiosis I prophase is required for accurate chromosome segregation to form euploid gametes. The repair of Spo11-induced double-strand breaks (DSB) using a homologous chromosome template is a major driver of pairing in many species, including fungi, plants, and mammals. Inappropriate pairing and crossing over at ectopic loci can lead to chromosome rearrangements and aneuploidy. How (or if) inappropriate ectopic interactions are disrupted in favor of allelic interactions is not clear. Here we used an *in vivo* “collision” assay in budding yeast to test the contributions of cohesion and the organization and motion of chromosomes in the nucleus on promoting or antagonizing interactions between allelic and ectopic loci at interstitial chromosome sites. We found that deletion of the cohesin subunit Rec8, but not other chromosome axis proteins (e.g. Red1, Hop1, or Mek1), caused an increase in homolog-nonspecific chromosome interaction, even in the absence of Spo11. This effect was partially suppressed by expression of the mitotic cohesin paralog Scc1/Mdc1, implicating Rec8’s role in cohesion rather than axis integrity in preventing nonspecific chromosome interactions. Disruption of telomere-led motion by treating cells with the actin polymerization inhibitor Latrunculin B (Lat B) elevated nonspecific collisions in *rec8Δ spo11Δ*. Next, using a visual homolog-pairing assay, we found that the delay in homolog pairing in mutants defective for telomere-led chromosome motion (*ndj1Δ* or *csm4Δ*) is enhanced in Lat B-treated cells, implicating actin in more than one process promoting homolog juxtaposition. We suggest that multiple, independent contributions of actin, cohesin, and telomere function are integrated to promote stable homolog-specific interactions and to destabilize weak nonspecific interactions by modulating the elastic spring-like properties of chromosomes.

Citation: Lui DY, Cahoon CK, Burgess SM (2013) Multiple Opposing Constraints Govern Chromosome Interactions during Meiosis. *PLoS Genet* 9(1): e1003197. doi:10.1371/journal.pgen.1003197

Editor: Michael Lichten, National Cancer Institute, United States of America

Received: November 11, 2010; **Accepted:** November 12, 2012; **Published:** January 17, 2013

Copyright: © 2013 Lui et al. This is an open-access article distributed under the terms of the Creative Commons Attribution License, which permits unrestricted use, distribution, and reproduction in any medium, provided the original author and source are credited.

Funding: This work was supported by a grant from the National Institutes of Health to SMB (RO1-GM075119) and from the Environmental Health Services Training Grant to DYL (NIH T32 ES07059). The funders had no role in study design, data collection and analysis, decision to publish, or preparation of the manuscript.

Competing Interests: The authors have declared that no competing interests exist.

* E-mail: smburgess@ucdavis.edu

^a Current address: Department of Genetics, Harvard Medical School, Boston, Massachusetts, United States of America

^b Current address: Stowers Institute for Medical Research, Kansas City, Missouri, United States of America

These authors contributed equally to this work.

Introduction

Meiosis is a specialized cell division program that generates haploid gametes from diploid parental cells. A hallmark of the meiosis I division is the reductional segregation of homologous chromosomes while the meiosis II division segregates sister chromatids. The reductional division requires crossing over between homologous chromosomes in combination with sister chromatid cohesion [1,2]. Errors preventing normal chromosome segregation are a major cause of birth defects and miscarriage [3].

Crossing over is the outcome of reciprocal exchange of chromosome segments of homologous nonsister chromatids. Typically exchange occurs at allelic positions on homologous chromosomes but can also occur erroneously between ectopic regions of homology located on nonhomologous chromosomes, resulting in deletions, insertions and/or translocations [4–7]. Over the past decade, major inroads have been made in understanding mechanisms that promote pairing between homologous chromosomes but little is known about the mechanisms that prevent nonallelic interactions [8]. Several lines of evidence point to the

sequestration of repeated elements to “silenced” regions near the nuclear periphery [7,9–11] or through engagement with allelic DNA sequences by homologous recombination [12,13].

The relationship between events that initiate crossing over and mechanisms that promote the side-by-side alignment of homologs varies among species [14]. In a majority of model organisms studied, including mouse, plants and fungi, the repair of Spo11-induced double-strand breaks (DSBs) using the homologous chromosome as a repair template is a major driver of pairing [15–23]. By contrast, in *Caenorhabditis elegans* and *Drosophila* females where recombination is still required for proper disjunction, homologs can pair even in the absence of meiotic-induced DSBs [24–26]. In *C. elegans*, pairing is initiated at pairing centers found at one end of each chromosome [27]. In *Drosophila* females, achiasmate chromosomes can pair via regions of heterochromatin [24,25,28]. In *Drosophila*, and to a lesser extent in budding yeast, an alternative mechanism to segregate achiasmate chromosomes exists that relies on homolog nonspecific interactions between centromere sequences [29–31].

Author Summary

Meiosis is the key stage of gametogenesis, when the diploid genome complement is reduced by one half to form haploid gametes for sexual reproduction. Accurate chromosome segregation requires that homologous chromosomes pair, recombine by crossing over, and segregate from one another during the first meiotic division. Missegregation of homologs leads to the formation of aneuploid gametes, while erroneous crossing over between ectopic chromosomal loci can lead to chromosomal rearrangements such as translocations and deletions. We found that nonspecific interactions between interstitial chromosomal sites can be enabled or prevented through multiple, independent mechanisms during meiosis in budding yeast. These include organization of chromosomes in the nucleus, integrity of the chromosome axis structure, and actin-led chromosome movement. Acting together, these processes can reinforce strong chromosome interactions that promote pairing, while acting in opposition they can eliminate weak nonspecific interactions. These data provide an integrated view of how homologous chromosome pairing is achieved.

While full levels of pairing in budding yeast *Saccharomyces cerevisiae* requires the formation and repair of DSBs there is also evidence for DSB-independent pairing both in vegetatively dividing cells and during meiosis in (e.g. in a *spo11Δ* mutant) [32–36]. The configuration of chromosomes with respect to centromere and/or telomere clustering and chromosome territories contributes in part to associations between homologous chromosomes at these regions [8,13,37,38]. Centromere coupling is an early event during meiotic prophase that involves pairwise associations of centromeres independent of homology [29,35]. Examples abound from a wide variety of species for somatic homolog pairing in higher eukaryotes with direct influence on gene expression or DNA repair [7,39].

The structural core of the meiotic chromosome axis in budding yeast comprises a conserved group of proteins, including Rec8, a meiosis-specific α -kleisin subunit of cohesin as well as Red1, Hop1 and Mek1 [40–46]. Inactivation of any of these proteins compromises interhomolog bias and homolog pairing [15,18,21,47–53]. Deletion of Rec8 also impacts several events of meiotic prophase not associated with sister chromatid cohesion, including region-specific distribution of Spo11 and DSB formation along chromosomes, meiotic S-phase timing, centromere coupling, synapsis, homolog pairing, transcription, and progression through meiotic prophase [40,44,49,51,54–58]. Rec8 also plays an important role in chromosome segregation at meiosis I by preventing premature sister chromatid separation prior to anaphase I [40].

In addition to the biogenesis of specialized chromatin architecture, meiotic chromosomes of nearly all species assume a polarized, nonrandom configuration in the nucleus, often with telomeres clustered toward one side of the nucleus [59]. This configuration is associated with vigorous telomere-led movement driven by cytoskeleton structures (either actin or microtubules depending on the species) outside the nucleus through protein bridges that span the inner and outer nuclear membranes and attach to telomeres [60,61]. In budding yeast, the velocity of telomere-led movement is greatest during late zygotene to pachytene stages when homologs are already paired, however, slower chromosome movement can be observed prior to zygotene during the pairing stage [62–65]. Chromosome organization and motion appear to be coupled to events associated with pairing and

recombination since nearly every mutation affecting one or both of these aspects also exhibits slow turnover of recombination intermediates and delayed pairing.

Meiotic chromosomes are mechanically linked to the cytoskeleton through the intact nucleus by a conserved SUN-KASH protein bridge [66,67]. Ndj1 is a fungal-specific telomere-associated protein that promotes telomere/NE associations [63,68–70]. Ndj1 interacts with the conserved SUN-protein Mps3 that spans the inner nuclear envelope [71]. Mps3 interacts with Csm4, a putative KASH protein with a single transmembrane tail domain bridging the outer nuclear envelope; Csm4 is required for telomeres to coalesce into the bouquet configuration and undergo Ndj1-dependent motion [63,64,72,73].

This work focuses on how the structure and organization of chromosomes in the nucleus impacts interactions between allelic and ectopic interstitial chromosomal loci. Here we carried out extensive epistasis analysis using deletion mutations in genes known to be involved in each of the functions described above to define the co-dependent or independent pathways leading to close-stable homolog juxtaposition (CSHJ). We applied an *in vivo* assay (*Cre/loxP*) that measures the relative spatial proximity/or accessibility of pairs of chromosomal loci [32]. Maximal levels of site-specific recombination between homologous chromosomes indicated close, stable homolog juxtaposition of the assayed interstitial loci [21]. Through the analysis of mutants defective for various processes related to meiotic recombination we found that early steps of homologous recombination, including strand invasion and single end invasion are major determinants of CSHJ, while synapsis plays a relatively minor role [21,74,75].

Results

The experimental system

To probe the spatial proximity and/or accessibility of pairs of interstitial chromosomal loci *in vivo*, we measured the frequency of Cre-catalyzed recombination between pairs of *loxP* sites located at allelic and ectopic chromosomal loci per meiosis. These sites were integrated at positions equidistant from the centromere and the adjacent telomere on the long arms of two average sized chromosomes (*V* and *VIII*; see Experimental Procedures for more details). Previously, we measured site-specific recombination events by selecting for prototrophs resulting from the coupling of a promoter region to a selectable reporter gene; prototrophs were recovered from synchronized meiotic cells plated on selective media by “return to growth” (RTG) at various time points after the initiation of meiosis (by transfer to sporulation medium; SPM [21]). In this study we measured recombinant DNA products by quantitative PCR using chromosome-specific primers flanking each *loxP* site (Figure 1A). One key advantage of using qPCR is that *Cre/loxP* recombination can be assessed in strains that do not survive RTG and processing samples is more efficient. Template DNA for PCR was isolated from cells collected 10 hours after the initiation of meiosis. The recombination events are normalized for each sample by dividing by the copy number of a control locus that does not undergo *Cre/loxP* recombination (*ACT1*). By multiplying the normalized value by the total number of chromatids per chromosome (four chromatids for most of the strains analyzed in this study), we generate the number of Cre-mediated recombination events per meiosis. The output of this assay, for both the RTG and qPCR method, is the frequency of *Cre/loxP* recombination events per meiosis, which we will refer to here as “collisions” (Figure 1A).

Strains used in this analysis carry an *ndt80Δ* mutation to prevent pachytene exit; blocking this late prophase step provides a control for differences in division timing and/or arrest exhibited by

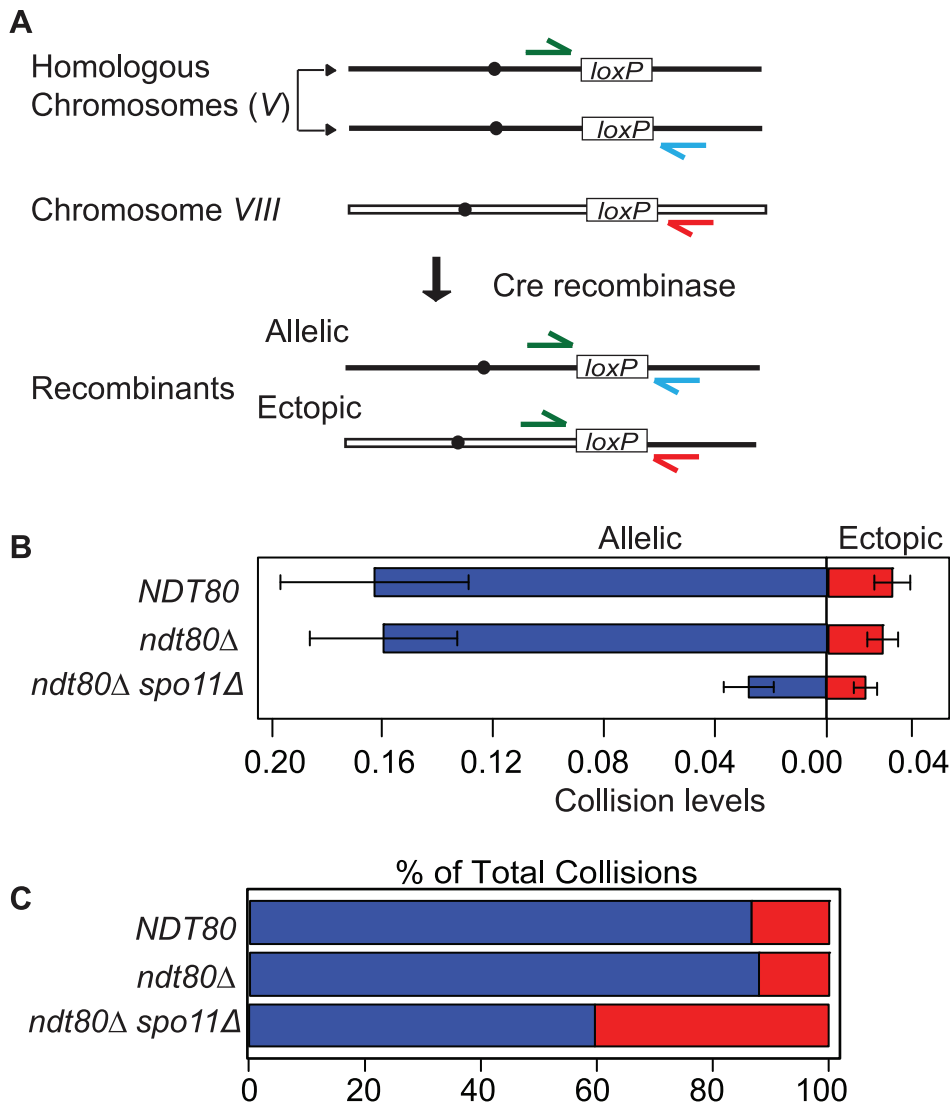


Figure 1. Inter-chromosomal collision assay. A. The chromosomal location of *loxP* sites for the collision assay described in the text. The primer configurations for detection of recombinants by qPCR are diagrammed. B. Comparison of average allelic and ectopic collision levels in *NDT80* versus *ndt80Δ* and *ndt80Δ spo11Δ*. Collisions are the measured level of recombinants per meiosis (i.e. 4 chromatids). The variance for allelic collision levels was somewhat higher than for ectopic. This may be due to differences in primer sequence and primer pair concentrations optimized for the respective qPCR reaction conditions; the template DNA isolated from each individual time course for both cases is the same. C. Percent of allelic collisions (blue) and ectopic collisions (red) among total collisions measured (allelic and ectopic). doi:10.1371/journal.pgen.1003197.g001

various meiotic mutants [76]. Prolonged arrest at pachytene does not affect the output of the assay since *NDT80* and *ndt80Δ* strains gave similar levels of both allelic and ectopic collisions (Figure 1B).

It is important to note that collision levels represent the cumulative events that occur from the time of bulk DNA replication, when Cre recombinase is induced by galactose addition, until a fixed arrest point prior to exit from pachytene. Galactose induction increased allelic and ectopic collision levels 100- and 350-fold compared to those in untreated cells, respectively (Table S1); thus, the dynamic range spans two orders of magnitude while background level of events is negligible.

Collision levels measured using the qPCR and RTG methods were in agreement: Allelic collision levels were 0.13 ± 0.03 and 0.14 ± 0.03 recombinants/4 chromatids for qPCR and RTG values, respectively; ectopic collision levels were 0.018 ± 0.004 and 0.015 ± 0.004 , respectively (Figure S1). From previous studies, we

have inferred that the elevated level of allelic versus ectopic collisions is due to homology-dependent interhomolog interactions in sequences outside the reporter locus [21,74,75,77]. A number of mutants defective for meiotic recombination including *spo11Δ*, *sae2Δ*, *rad51Δ*, and *rad52Δ* exhibited reduced allelic collision levels compared to wild type when measured by qPCR and RTG assays (Figure S1). Additional mutants defective for biochemical aspects of recombination including *zip3Δ*, *rdh54Δ*, and *sgs1-mn* (a meiotic null allele of *SGS1*) were analyzed in the course of this study but not discussed here (Figures S2, S3 and Table S2; [78–83]).

Rec8 promotes allelic collisions independent of its role in sister chromatid cohesion

Rec8 plays dual roles during meiotic prophase; the first is to mediate sister chromatid cohesion and the second as a structural component of the chromosome axis that regulates the position and

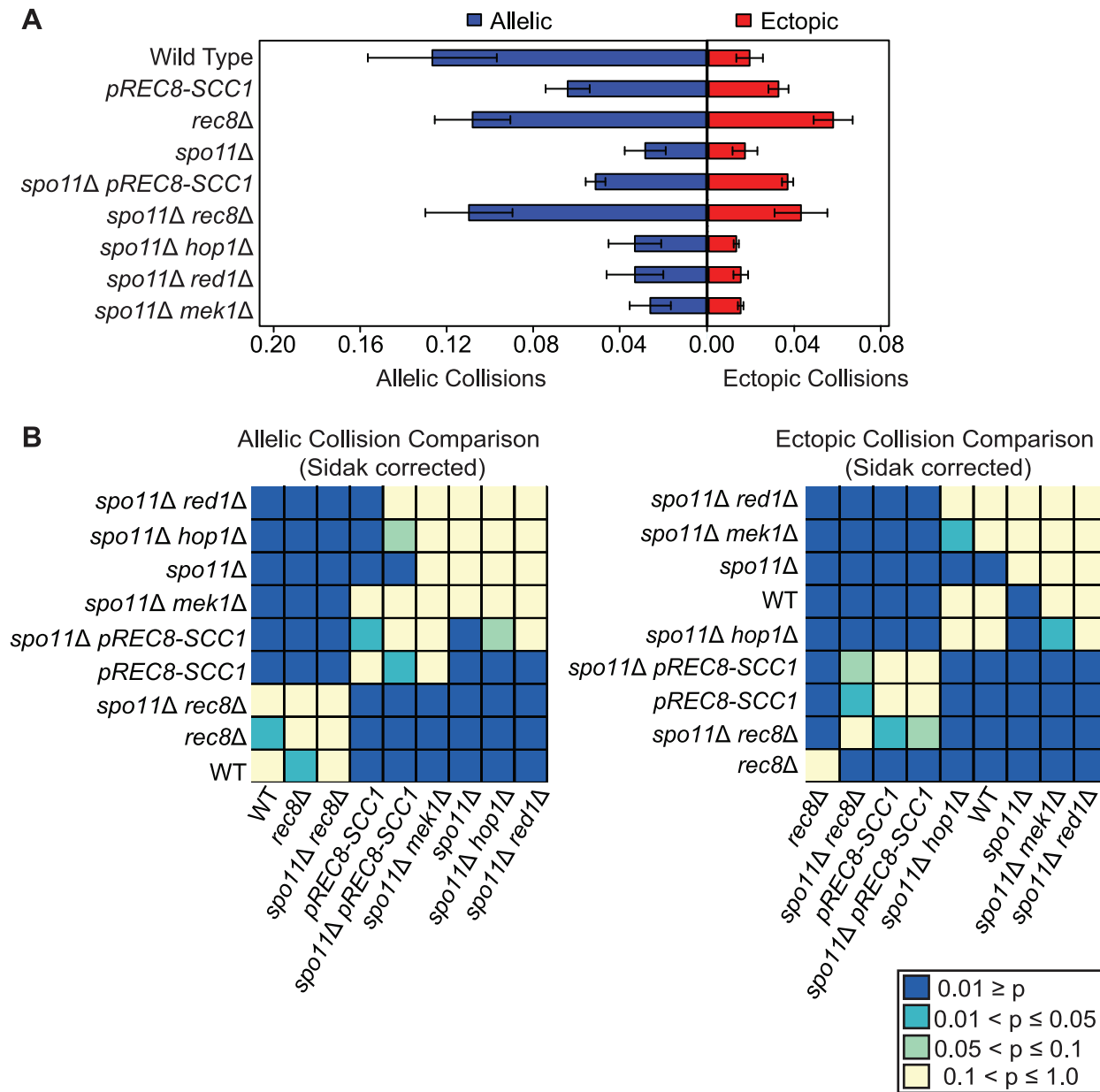


Figure 2. Rec8 promotes allelic collisions independent of its role in sister chromatid cohesion and prevents nonspecific collisions. A. Analysis of allelic and ectopic collision levels as described in Figure 1. B. Heatmap of Sidak adjusted *P*-values comparing collision levels between all allelic collision levels (left) and all ectopic collision levels (right). doi:10.1371/journal.pgen.1003197.g002

outcomes of homologous recombination (Introduction). To explore if one or both of these functions influence the proximity and/or accessibility of interstitial chromosomal loci, we measured allelic and ectopic collision levels in a strain expressing the mitotic cohesin *SCC1/MCD1* in place of *REC8* (*pREC8-SCC1*) in the *rec8Δ* mutant. In *pREC8-SCC1*, sister chromatid cohesion is maintained while meiosis-specific functions, including chromosome axis and SC assembly are absent [49,56,84]. In *rec8Δ* mutants, both aspects of Rec8 function are absent.

We found that *pREC8-SCC1* reduced the level of allelic collisions 2-fold compared to wild type (0.064 ± 0.009 versus 0.127 ± 0.031 , $P < 0.00001$; Figure 2) implicating a role for Rec8 in promoting allelic chromosome interactions independent of its role in sister chromatid cohesion. Brar *et al.* reached a similar conclusion by

analyzing pairing in individual cells using GFP-tagged chromosomes in this mutant background [49]. To our surprise, we found that the level of allelic collisions and ectopic collisions in *rec8Δ* (i.e. the absence of cohesion) was greater than in the *pREC8-SCC1* ($P = 6.04e^{-11}$; Figure 2). In addition, the level of ectopic collisions was elevated 3-fold in the *rec8Δ* mutant compared to wild type (0.058 ± 0.009 versus 0.019 ± 0.006 , $P = 1.04e^{-13}$) and *pREC8-SCC1* (0.058 ± 0.009 versus 0.032 ± 0.004 , $P = 3.43e^{-9}$). Together these results suggest that Rec8 promotes interhomolog interactions and suppresses ectopic interactions, and perhaps nonspecific allelic interactions (below). These effects may be region-specific since the regions including *FLO8* (*V*) and *NDT80* (*VIII*) are enriched for Rec8 binding and exhibit decreased levels of DSBs in *rec8Δ* mutant cells compared to wild type [85–87].

Nonspecific collisions are elevated in both *rec8Δ* and *pREC8-SCC1* mutants

We reasoned that the relatively modest reduction in the allelic collision level conferred by *rec8Δ* compared to *pREC8-SCC1* might be due to the inclusion of a significant fraction of “nonspecific” interactions (i.e. those occurring in the absence of homology-dependent interactions). To test this, we measured the level of collisions in a *spo11Δ* mutant background since homologous recombination is a major driver of allelic collisions in wild type strains [75]. We found that the level of allelic collisions in *spo11Δ rec8Δ* was 3.9-fold greater than in the *spo11Δ* single mutant (0.110 ± 0.020 versus 0.028 ± 0.009 , $P = 1.49e^{-11}$ respectively; Figure 2). Allelic collisions in *spo11Δ pREC8-SCC1* were also greater than *spo11Δ* (2-fold; 0.055 ± 0.011 versus 0.028 ± 0.009 , $P = 1.72e^{-5}$ respectively; Figure 2), but to a lesser extent than *spo11Δ rec8Δ*. Likewise, ectopic collision levels were elevated in *spo11Δ rec8Δ* and *spo11Δ pREC8-SCC1* compared to *spo11Δ* ($P = 0.0003$ and $P = 7.88e^{-9}$, respectively; Figure 2). This trend was also observed, but to a lesser extent, in a *spo11Δ rec8Δ cdc6-mn* where cells progress through meiosis without fully duplicating the parental chromosomes (Figures S2 and S3; [88]). These results suggest that the loss of Rec8 cohesion function (but not loss of sister cohesion *per se*) leads to increased interactions between chromosomal loci independent of DSB formation.

Nonspecific collisions are not elevated in the absence of Red1, Hop1, or Mek1

We next tested if other components of the meiotic chromosome axis (Red1, Mek1 and Hop1) limit nonspecific collisions similar to Rec8. Unlike the case for *spo11Δ rec8Δ*, however, we found that the levels of allelic and ectopic collisions in *spo11Δ red1Δ*, *spo11Δ mek1Δ* and *spo11Δ hop1Δ* mutants were indistinguishable from *spo11Δ*, with the exception of *spo11Δ hop1Δ* in which ectopic collision levels were slightly reduced ($P = 0.005$; Figure 2). These results further indicate that the effect of the *rec8Δ* on increasing chromosome interactions is due the absence of cohesin and not by disrupting the core axis structure.

The increase in nonspecific collisions in *rec8Δ* is not due to the persistent bouquet

We next tested the possibility that the relatively high level of nonspecific chromosome interactions in *spo11Δ rec8Δ* is due to the juxtaposition of loci located at similar chromosomal “latitudes” in the bouquet configuration since the bouquet persists in this mutant background [53]. We reasoned that disrupting the bouquet might reverse the increased levels of nonspecific interactions conferred by *rec8Δ*. To test this we deleted *NDJ1*, encoding a telomere-associated protein that promotes attachment of chromosome ends to the nuclear envelope, and assayed collisions under this condition where the bouquet is absent [70,73,89]. We found that the levels of both allelic and ectopic collisions were similar in *spo11Δ rec8Δ ndj1Δ* and *spo11Δ rec8Δ* ($P = 0.3$ and $P = 0.8$ respectively) suggesting that a persistent bouquet is not responsible for increased collision levels in the *rec8Δ* background (Figure 3). Interestingly a significant reduction in ectopic collisions was found in the control strain *spo11Δ ndj1Δ* compared to *spo11Δ* (0.012 ± 0.004 and 0.017 ± 0.006 respectively, $P = 0.003$; Figure 3). This finding was further explored as described below.

Addition of the actin polymerization inhibitor Lat B further increases nonspecific collisions in *spo11Δ rec8Δ*

We next speculated that the high levels of nonspecific interactions observed in *spo11Δ rec8Δ* might be driven by actin-mediated motion.

To test this, we added the actin polymerization inhibitor Latrunculin B (Lat B) to cell synchronized meiotic cultures and asked if it reduced the levels of allelic and ectopic collisions [90]. We were surprised to find that the level of allelic collisions was instead increased in *spo11Δ rec8Δ* cells treated with Lat B compared to untreated cells (0.140 ± 0.010 vs. 0.110 ± 0.020 ; $P = 1.9e^{-5}$). This trend was also observed for ectopic loci (0.047 ± 0.008 vs. 0.043 ± 0.012 , albeit above the threshold of significance; Figure 3). This outcome suggests that actin can antagonize nonspecific interactions. There was no measurable effect of Lat B on the *spo11Δ* single mutant. Moreover, Lat B treatment did not significantly affect the level of allelic collisions in the *pREC8-SCC1 spo11Δ* mutant where sister chromatid cohesion exists (Figure 3). These results suggest that the cohesin function of Rec8 acts in opposition to an actin-based mechanism to suppress nonspecific chromosome interactions.

If the elevated level of nonspecific interactions in *spo11Δ rec8Δ* were due to Ndj1-dependent, telomere-led motion we would expect that the addition of Lat B to *spo11Δ rec8Δ ndj1Δ* would have no effect. Instead, we found that Lat B elevated both allelic collisions (0.143 ± 0.016 versus 0.095 ± 0.017 ; $P = 0.0001$; Figure 3) and ectopic collisions (0.051 ± 0.002 versus 0.037 ± 0.007 ; $P = 0.0002$; Figure 3) by approximately 50% even in the absence of Ndj1. Without the combined constraints of Ndj1-dependent attachment of chromosomes to the nuclear envelope, Rec8-mediated cohesion and an unknown feature of actin (i.e. Lat B treated *spo11Δ rec8Δ ndj1Δ*), the total level of collisions (i.e. the sum of allelic and ectopic events) is 4.3 fold greater than when these constraints are intact (i.e. in a *spo11Δ* single mutant). Thus, even in the absence of DSBs, multiple independent processes appear to impose chromosome order within the 3D space of the nucleus.

Addition of Lat B elevates allelic collisions in *csM4Δ* and *ndj1Δ* mutants

The addition of Lat B to wild-type cells does not affect overall levels of homolog pairing assayed using FISH, however, it delays the kinetics of pairing compared to untreated cells [53]. When Lat B was added to wild type (e.g. *SPO11*) cells the level of allelic collisions was modestly reduced to 84% of untreated cells ($P = 0.003$; Figure 4) the level of ectopic collisions remained unchanged ($P = 0.2$; Figure 4), suggesting that actin can play a positive role in promoting recombination-mediated allelic interactions in addition to antagonizing nonspecific interactions (above). This result is not surprising since the levels of crossover-bound recombination intermediates (Single End Invasions (SEIs) and double Holliday Junctions (dHJs)) are not dramatically reduced in Lat B-treated cells [62].

By contrast, we found that the addition of Lat B increased levels of allelic collisions in *rec8Δ*, *ndj1Δ*, *csM4Δ*, *rec8Δ ndj1Δ* and *ndj1Δ csM4Δ* compared to untreated cells (Figure 4). These results suggest that in the absence of telomere-led movement or dynamic nuclear deformations, a Lat B sensitive process can negatively influence allelic chromosome interactions. Interestingly, only *rec8Δ* and *rec8Δ ndj1Δ* mutants significantly increase ectopic collision levels and Lat B further increases these collisions ($P = 0.02$; $P = 0.0004$ respectively, Figure 4). These results are consistent with the findings shown above (Figure 3) suggesting a role for Rec8 in constraining nonspecific chromosome interactions. Moreover, these data implicate actin in a nuclear process independent of Ndj1-dependent telomere-led motion.

Lat B disrupts pairing of GFP-tagged chromosomal loci in wild type, *ndj1Δ*, and *csM4Δ*

We next used an independent visual assay to measure the effect of Lat B on chromosome interactions using strains expressing a

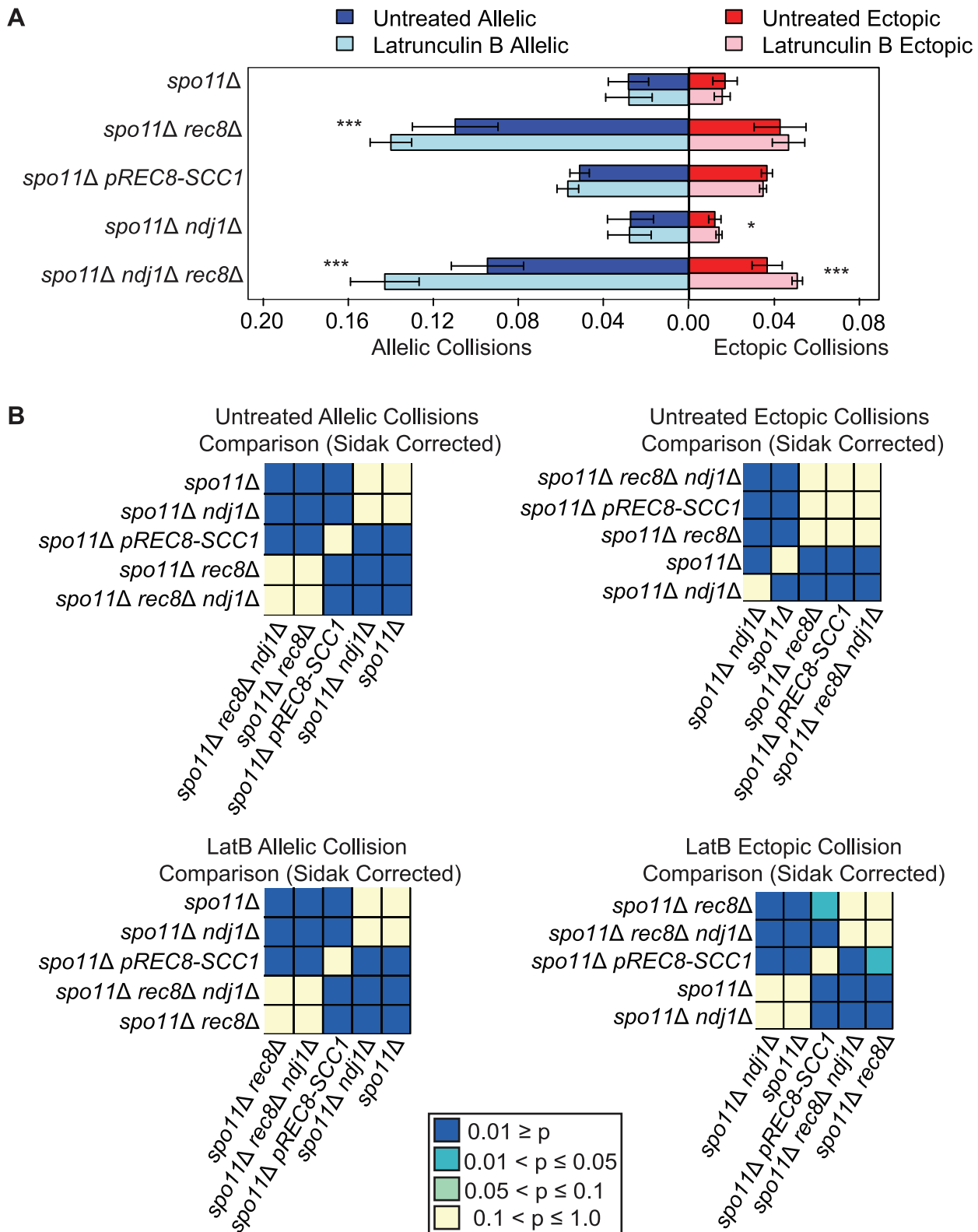


Figure 3. Elevated levels of nonspecific collisions in *rec8Δ* mutants do not require recombination initiation. A. Analysis of collisions in *spo11Δ*, *spo11Δ rec8Δ*, *spo11Δ prec8-SCC1*, *spo11Δ ndj1Δ*, and *spo11Δ ndj1Δ rec8Δ* mutants with Lat B treatment. Allelic (blue) and ectopic (red) collision levels in untreated cultures (dark bars) and Lat B treatment (light bars). Asterisks denote significant differences as follows: (*), *P*-values between 0.05 and 0.01; (**), *P*-values between 0.01 and 0.001; (***), *P*-values <0.001 by a two-tailed Student's *t*-test. B. Heatmap of Sidak adjusted *P*-values from Student's *t*-test comparing collision levels between relevant mutants in untreated and Lat B treated cells.
doi:10.1371/journal.pgen.1003197.g003

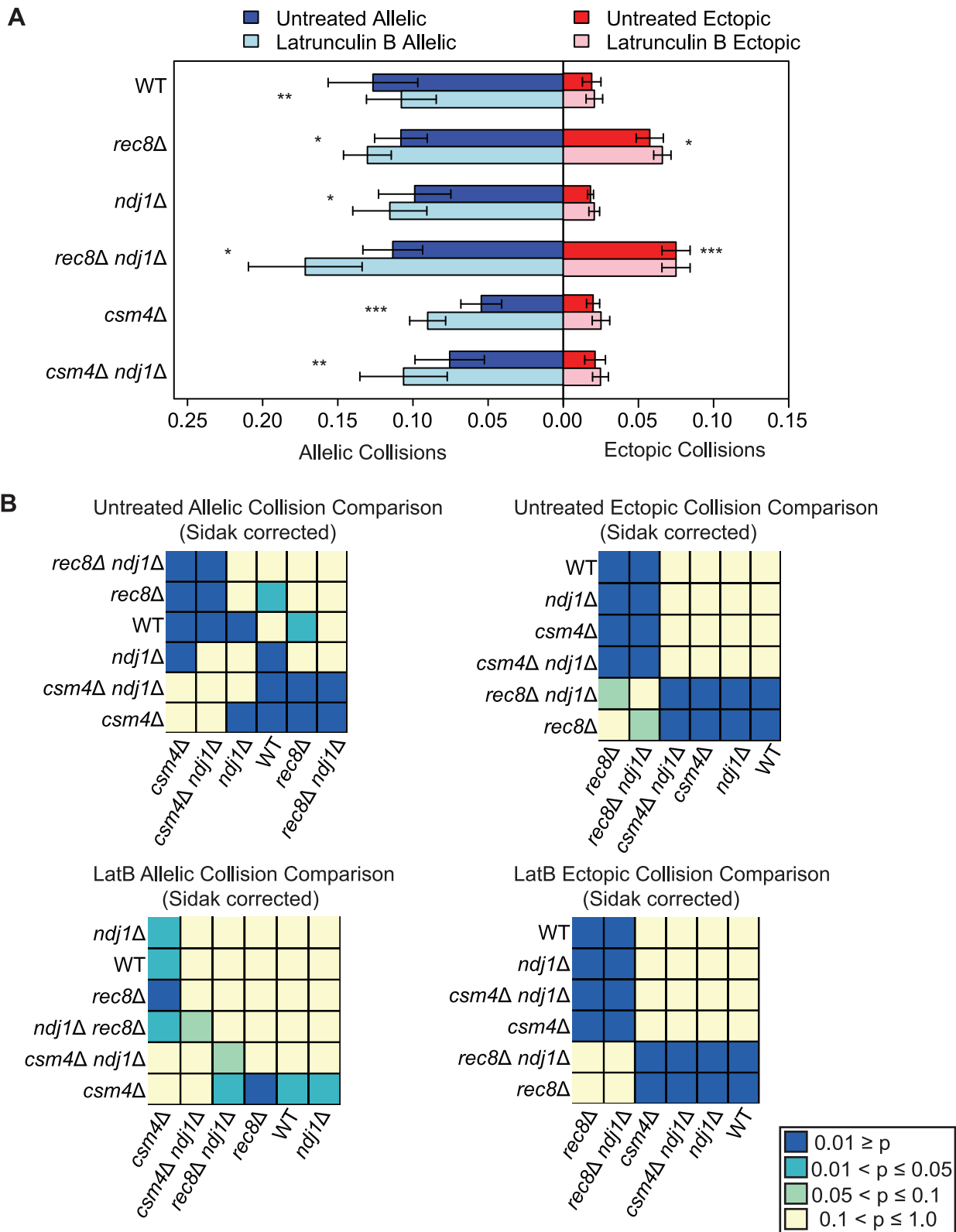


Figure 4. Elevated levels of nonspecific collisions in *rec8Δ* do not require *Ndj1*-dependent telomere attachments to the NE. A. Analysis of allelic and ectopic collision levels in *rec8Δ*, *ndj1Δ*, *ndj1Δ rec8Δ*, *csm4Δ*, and *ndj1Δ csm4Δ* mutants with Lat B treatment. Graph parameters are as described as in Figure 3. B. Heatmap of Sidak adjusted *P*-values from Student's *t*-test comparing collision levels between relevant mutants in untreated and Lat B treated cells.
doi:10.1371/journal.pgen.1003197.g004

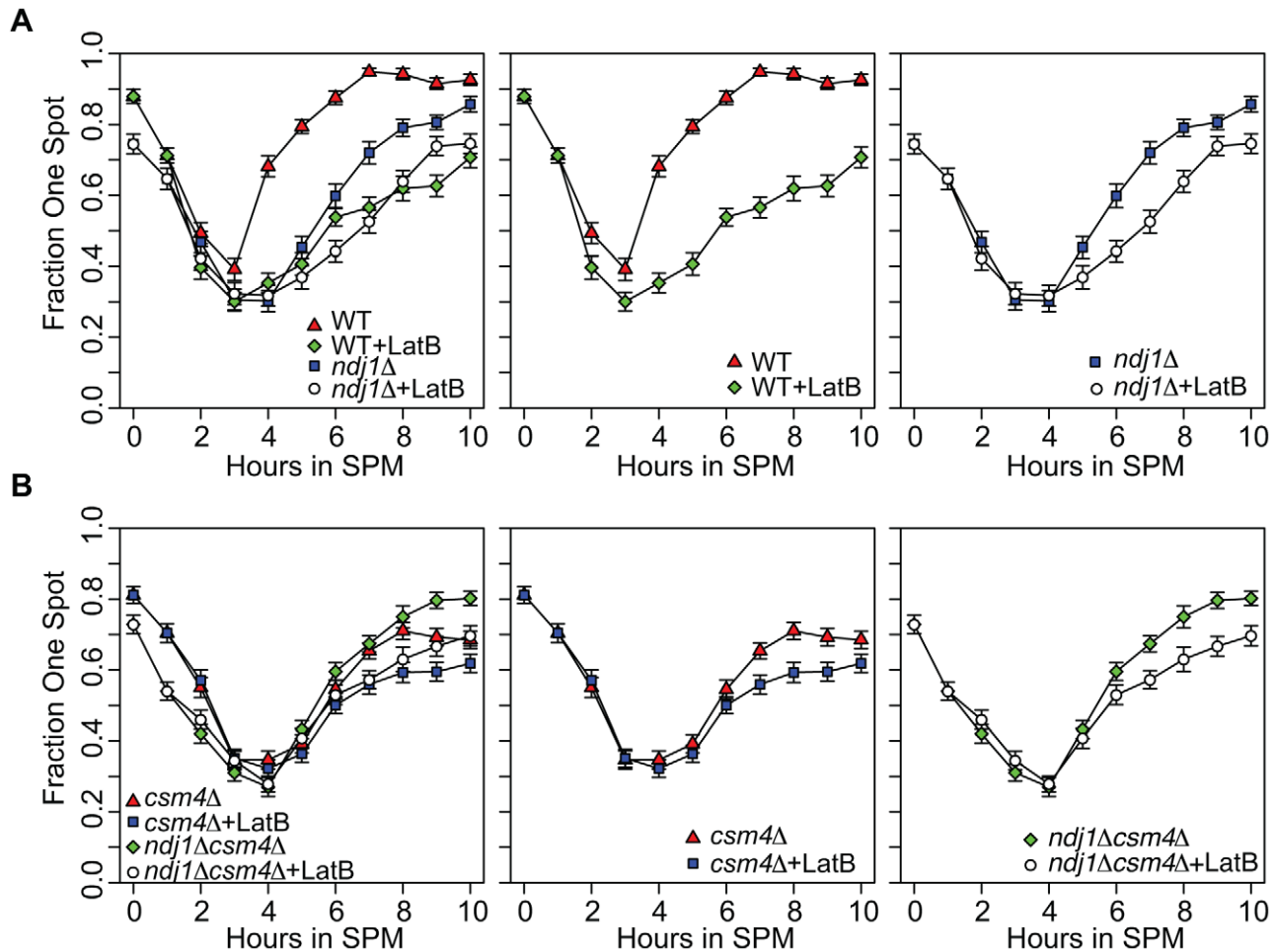


Figure 5. Homolog pairing kinetics in wild-type, *ndj1* Δ , *csm4* Δ , and *ndj1* Δ *csm4* Δ cells with and without Lat B treatment. Kinetics of pairing in cells with *tetO* arrays integrated at *URA3*, located 35 kb away from the centromere on chromosome V, and expressing *tetR*-GFP fusion protein. Homologs are considered paired if only one GFP can be visualized in the cells ($n=200$) from each time point. Error bars represent the standard error of the percentage of cells paired for independent cultures for each mutant ($n=200$). All strains carry the *ndt80* Δ mutation. A. Analysis of WT (center panel and left panel) and *ndj1* Δ (right panel and left panel) pairing kinetics in the presence or absence of Lat B. B. Analysis of *csm4* Δ (center panel and left panel) and *ndj1* Δ *csm4* Δ (right panel and left panel) pairing kinetics in the presence or absence of Lat B. doi:10.1371/journal.pgen.1003197.g005

TetR-GFP fusion protein that binds integrated *tetO* arrays at the *URA3* locus on homologous chromosomes [91–93]. As was also observed by Brar *et al.*, for wild type, the two loci colocalize forming one focus prior to transfer of cells to SPM. As cells enter meiosis, colocalization is progressively reduced up until about $t=3$ hours (Figure 5A; [49]). While untreated cells reach maximum levels of pairing by $t=7$ hours ($\sim 90\%$ have one GFP spot; Figure 5A), pairing in Lat B treated cells was delayed and only $\sim 55\%$ had one spot at this time point. Thus, the effect of Lat B on pairing using this visual assay was more severe than using the collision assay.

Pairing kinetics in the untreated *ndj1* Δ mutant were delayed compared to wild type, similar to observations made using FISH [70]. This delay was even greater in Lat B-treated cells. Indeed, the kinetics of pairing in both wild type and *ndj1* Δ cells treated with Lat B were similar (Figure 5A). These results suggest 1) Ndj1 does not play a role in promoting pairing other than through its actin-related function and 2) that actin promotes pairing of allelic sites, in part, through a process that acts independently of Ndj1. We did not observe a recapitulation of the collision phenotype where Lat B stimulates allelic

collisions. Since the effect of Lat B appears to have an opposite effect in the GFP assay compared to the collision assay in the *ndj1* Δ , it is apparent that they measure different aspects of meiotic chromosome dynamics.

In the absence of Ndj1, there is a considerable degree of Lat B-sensitive dynamic nuclear deformation [94]. Since dynamic nuclear deformations require the putative KASH protein, Csm4 [94], we reasoned that addition of Lat B to *csm4* Δ or *csm4* Δ *ndj1* Δ would have little or no effect on the kinetics or absolute levels of pairing. This turned out not to be the case, however, since addition of Lat B reduced and/or delayed pairing levels in both mutants (Figure 5B). Together, these results suggest that an actin-mediated process and/or structure positively influences homolog pairing independent of Ndj1-dependent telomere-led motion or dynamic nuclear deformations.

Ndj1 and Zip1 together promote interactions between ectopic chromosomal loci in the absence of DSBs

During early meiotic prophase, chromosomes in yeast are loosely organized by centromere coupling and attachment of telomeres to the nuclear envelope. Since this configuration does

not require DSB formation, one widely held notion is that this arrangement of chromosomes may precede and set the stage for DSB-mediated pairing, similar to DSB independent pairing of heterochromatin in *Drosophila* or pairing centers in *C. elegans* [14,35,95,96]. We reasoned that collision levels might reflect this organization and that disruption of telomere attachment (e.g. *ndj1Δ*) and/or centromere coupling (e.g. *zip1Δ*) would reduce ectopic collision levels. To overcome the strong effects of homologous recombination, we carried out the analysis in a *spo11Δ* mutant background. Interestingly, ectopic collision levels were reduced in both the *spo11Δ ndj1Δ* and *spo11Δ zip1Δ* double mutants to 73% ($P=0.003$) and 75% ($P=0.03$) of *spo11Δ* levels, respectively (Figure 6). Notably, these are the only mutant situations for which we have observed a reduction in ectopic collisions either in the presence or absence of DSBs for dozens of analyzed mutant strains (Figure S2; [21,74,75]).

If the observed decrease in ectopic collision levels was due to the independent contributions of Ndj1 and Zip1, we expected that the *spo11Δ zip1Δ ndj1Δ* triple mutant would give even lower collision levels compared to either *spo11Δ ndj1Δ* or *spo11Δ zip1Δ* double mutants. Interestingly, however, ectopic collision levels in double and triple-mutant strains were indistinguishable ($P>0.99$ for both cases; Figure 6). These collision levels (~ 0.013) are two orders of magnitude above the lower limit of detection using this assay (i.e. $P<0.00005$; see Table S1), so a decrease should be detectable, in principle. These data suggest that Ndj1 and Zip1 participate in a single process that facilitates a subset of interactions between ectopic interstitial loci. For example, the simultaneous occurrence of telomere/NE tethering and centromere coupling could promote alignment of similar-sized chromosome arms, irrespective of homology. To further test this model, collisions at additional chromosomal sites must also be analyzed.

Evidence for weak forces destabilized by actin

To our surprise, Lat B added to *spo11Δ ndj1Δ* and *spo11Δ zip1Δ* double mutants restored ectopic collision levels to the same as *spo11Δ* (1.22-fold, $P=0.04$ and 1.37-fold, $P=0.003$, respectively). This was also true when Lat B was added to the *spo11Δ zip1Δ ndj1Δ* triple mutant (1.33-fold, $P=0.01$). By contrast, ectopic collisions in *spo11Δ* were virtually the same in untreated and treated cells (0.0173 ± 0.006 vs. 0.0154 ± 0.004 ; $P=0.11$, respectively; Figure 6 light blue bars). Thus, there appear to be weak stabilizing forces between ectopic sites maintained in the absence of Ndj1 and/or Zip1 that are sensitive to disruption by an actin mediated process or event.

We next tested if dynamic nuclear deformations are responsible for disrupting these weak ectopic interactions by introducing the *csn4Δ* mutation into these strains. In this case we would expect that the *csn4Δ* mutation would prevent destabilization and thus phenocopy the effect of Lat B treatment. This indeed turned out to be the case since ectopic collisions in *spo11Δ ndj1Δ* were increased to *spo11Δ* levels in the absence of Csm4 ($P=0.94$; Figure 6). Importantly, addition of Lat B to *spo11Δ csn4Δ* and the *spo11Δ ndj1Δ csn4Δ* triple mutant did not increase ectopic collisions indicating that Csm4 acts in the same pathway as an actin-mediated process (perhaps by mediating dynamic nuclear deformations) that destabilizes weak interactions between ectopic loci.

Discussion

Our goal was to understand how the nonrandom organization of chromosomes in the nucleus, including the contributions of actin-driven motion, promotes stable homolog juxtaposition and/or limits nonspecific interactions during meiosis prophase I. We used a quantitative “collision” assay to measure the relative

proximity and/or accessibility of allelic and ectopic pairs of interstitial chromosomal loci in various mutant strains of yeast defective for aspects of meiotic chromosome dynamics. We expanded the scope of our previous studies demonstrating that the repair of meiosis-induced DSBs plays a prominent role in achieving close, stable homolog juxtaposition [21,74,75]. We found evidence that supports roles for Ndj1/Csm4 and actin-driven motion in homolog pairing. We found that a combined function of Ndj1/Zip1 facilitates nonspecific chromosome interactions, perhaps by aligning similarly sized chromosomes engaged simultaneously in centromere coupling and telomere/NE attachment. Finally, we uncovered several independent mechanisms that antagonize nonspecific chromosome interactions, including a cohesion function of Rec8 and more than one process involving actin. We propose that close, stable homolog juxtaposition in yeast is achieved through a balance of forces that promote strong homolog specific interactions and destabilize (or prevent) weak nonspecific interactions. The discussion below describes how these multiple opposing forces are integrated to accomplish pairing and alignment of homologous chromosomes.

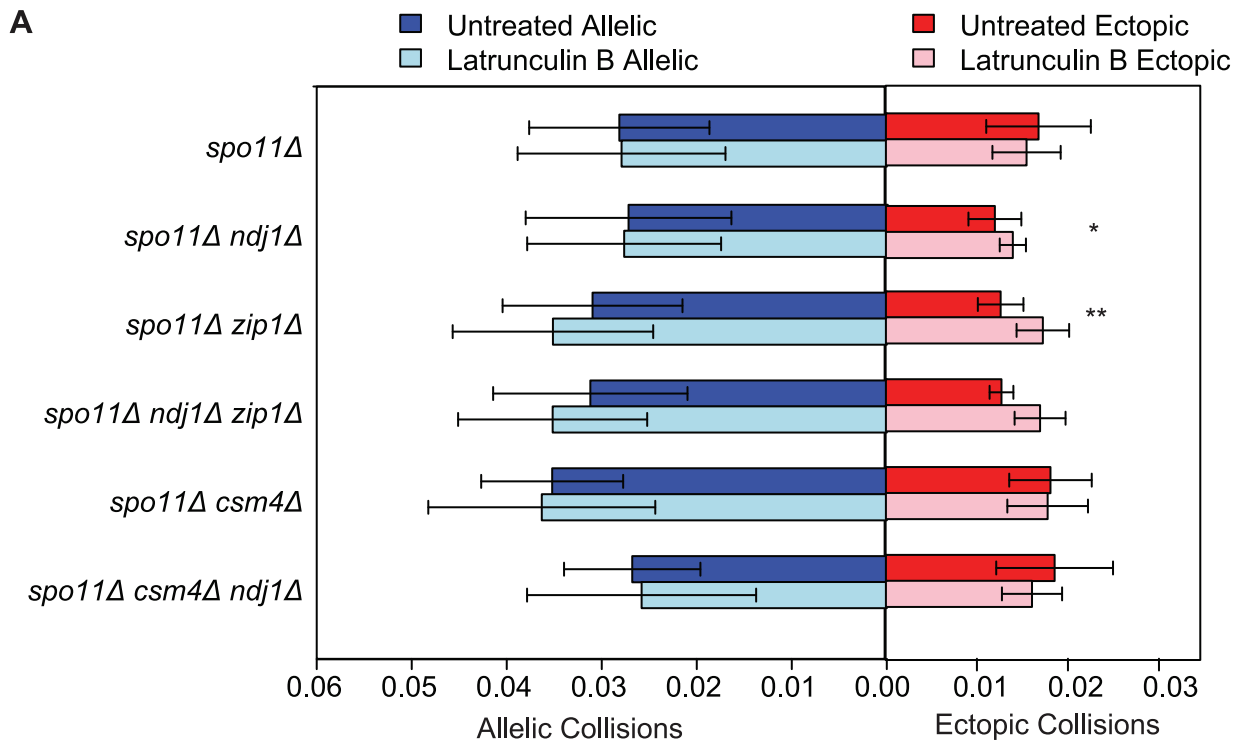
Ndj1 and Csm4 support homolog pairing through actin-directed motion

Rapid prophase movement of chromosomes is a prominent feature of mid-to-late meiotic prophase, yet little is known about the impact of chromosome motion during early meiotic prophase when chromosomes undergo pairing. We found that by eliminating one or all of three key components required for rapid prophase movement (Ndj1, Csm4 and actin polymerization) the kinetics of homolog pairing was delayed, consistent with findings using FISH and one-spot/two-spot TetR-GFP assays [64,70]. In addition, we found that wild type and *ndj1Δ* cells gave indistinguishable pairing levels in the presence of the actin polymerization inhibitor Lat B, suggesting that the contribution of Ndj1 to pairing occurs entirely through its role in actin-directed chromosome movement. Conversely, we found that Lat B caused a more severe pairing delay in *ndj1Δ* and *csn4Δ* mutants compared to untreated cells, also suggesting that actin may play roles in chromosome pairing independent of Ndj1 and Csm4 (see below).

We suggest that actin-independent motion (perhaps diffusion or changes in chromatin compaction) is sufficient for allowing chromosome pairing, but that the process is accelerated when chromosomes are actively moving. In *C. elegans*, where pairing does not rely on DSB repair, homolog pairing appears to be driven by a combination of dynein-driven motion and diffusion that initiates at pairing centers [97]; while the loss of active pairing center motion leads to pairing delays, diffusion-based motion is sufficient for pairing [97,98]. In *S. pombe*, mutations that disrupt dynein-driven nuclear movement of chromosomes also decrease the efficiency of the pairing process [20,99–101]. We suggest an analogous situation occurs in budding yeast except that actin-mediated forces are involved. Some recent studies have drawn similar conclusions [102,103].

Actin can antagonize chromosome interactions

While the outcomes of our one-spot/two-spot TetR-GFP visual assay indicate a positive role for actin in pairing independent of Ndj1/Csm4, outcomes from the collision assay indicated that actin might also prevent or destabilize nonspecific interactions. That is, in the absence of Ndj1 and/or Csm4, we observed that Lat B increased allelic collisions yet slowed the process of pairing. One way to reconcile these two observations is that spurious or nonproductive interactions may be destabilized by actin-mediated mechanism not related to Ndj1/Csm4-dependent motion. While



B Untreated Ectopic Collision Comparison (Sidak corrected)

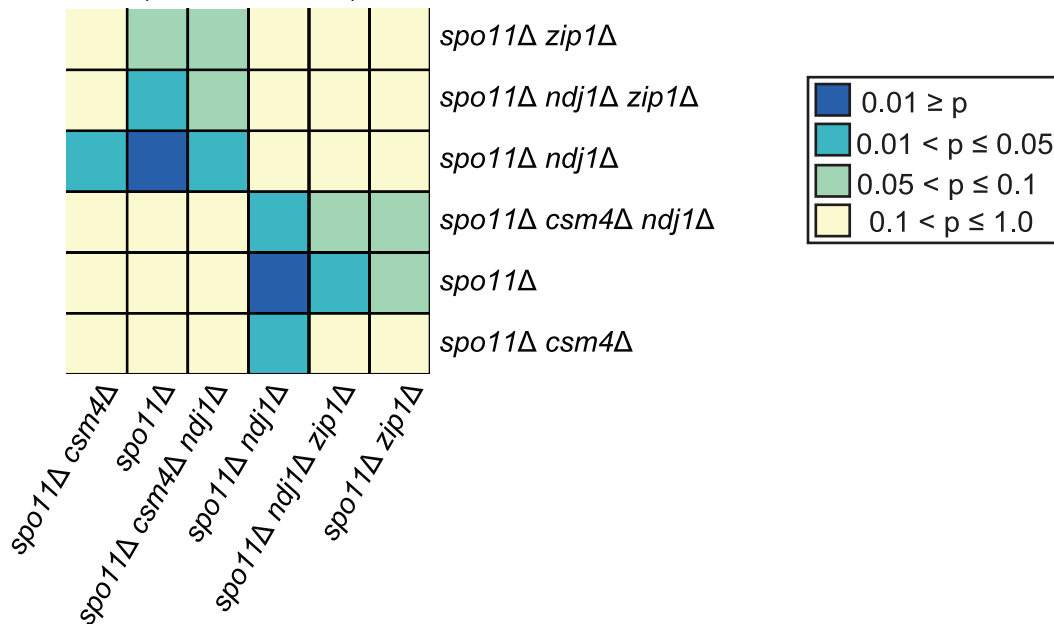


Figure 6. DSB-independent ectopic collision levels in mutants with defects in centromere coupling and bouquet formation. A. Analysis of collisions in *spo11Δ*, *spo11Δ ndj1Δ*, *spo11Δ zip1Δ*, *spo11Δ ndj1Δ zip1Δ*, *spo11Δ csm4Δ* and *spo11Δ csm4Δ ndj1Δ* mutants with Lat B treatment. Graph parameters are as described in Figure 3. B. Heatmap of Sidak adjusted *P*-values from Student's t-test comparing collision levels between relevant mutants in untreated and Lat B treated cells. doi:10.1371/journal.pgen.1003197.g006

the nature of this mechanism is not clear, one possibility is that interstitial chromosomal sites are subject to motion via the actin cables that surround the nucleus using a KASH protein complex other than Csm4 (and Ndj1) [62]. Alternatively, interaction

between interstitial chromosome sites might be prevented by sequestering them in different nuclear compartments and/or the nuclear envelope by association with an actin-associated structure or nuclear localized actin [104]. In interphase cells of yeast and

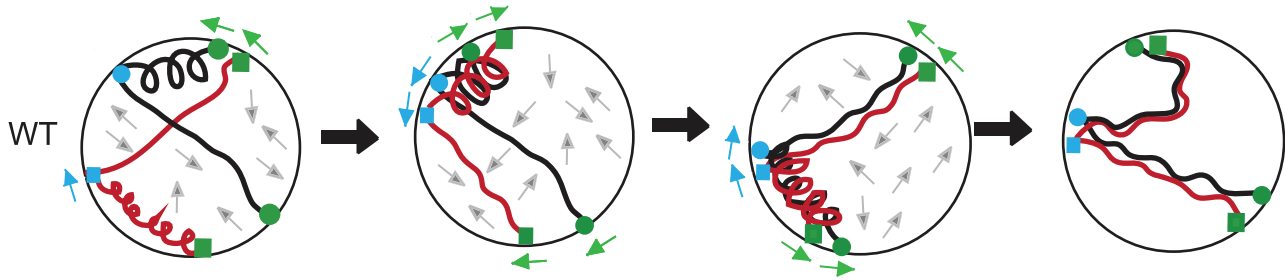


Figure 7. A mechanical model for homolog pairing. A hypothetical sequence of interactions between homologous chromosomes (shown as black or red) subjected to a coupled-spring oscillator (see text). In the sequence from left to right, homolog pairing becomes progressively stabilized as weak interactions are disrupted. The positive and negative forces of actin influence both homologs, with actin-based associations shown at telomeres (green; squares for the red chromosome and circles for the black homologous chromosome) and at interstitial sites (blue; squares for the red chromosome and circles for the black homologous chromosome). Arrows around the periphery of the nucleus indicate direction of movement for the telomeres (green) and the interstitial sites (blue). Grey arrows in the interior of the nucleus show “Brownian-like” motion/unknown forces on the chromosomes [105,119]. (i) In wild-type cells, segments of chromosomes that are in closer proximity have axial segments that are more compact. (ii) Compact segments of homologous chromosomes interact. (iii) Movement of chromosome attachment points on the nuclear envelope results in stretching of segments that remove unstable interactions between chromosomes. (iv) Stable interactions between allelic loci are those achieved up to the point of dHJ resolution as established using the Cre/*loxP* assay [21]. doi:10.1371/journal.pgen.1003197.g007

Drosophila, diffusive motion of chromosomes is constrained to a limited subregion of the nucleus and treatment with the microtubule depolymerizing agent nocodazole alleviates this confinement [105]. Perhaps, during yeast meiosis an actin-mediated process acts similarly to constrain interstitial chromosome loci to enhance pairing. Additionally, several nuclear processes including chromatin remodeling have been shown to require actin and/or sensitivity to Lat B [106–108]. Chromatin remodeling may be necessary for stable pairing of loci but may not be essential for their collision.

Multiple opposing forces promote strong interactions and eliminate weak interactions

We can envision a scenario where interstitial chromosome sites are coupled to one or more actin-based assemblies and their adjacent telomeres are attached to cytoplasmic actin cables via the Ndj1/Mps3/Csm4 protein bridge (Figure 7; Figure S4). The two systems acting simultaneously could direct discordant movement between chromosomes such that strong interactions persist while weak interactions are taken apart (Figure 7). Over time, chromosomes would be subject to alternating scrunching and stretching, perhaps analogous to a coupled-spring oscillator. Initially, chromosomes might undergo oscillations independent of one another, increasing the likelihood of productive strand invasion events to promote close, stable homolog juxtaposition. When pairing has been mostly achieved by zygotene [59], rapid prophase movement could serve to remove chromosome interlocks [60].

Evidence for a Rec8-dependent spring component in regulating chromosome interactions

One of the most surprising findings in our study was the high level of allelic and ectopic chromosome interactions observed in the absence of Rec8, even in a *spo11Δ* background. To better understand this result, mechanistic insight may be gained by considering the function of “SMCs” (cohesins and condensins) in distributing spindle-pulling forces across the pericentromeric chromatin loops during mitosis [109]. Bloom and colleagues describe SMCs as having the physical attributes of “slip rings” (molecular pulleys) that impart the distribution of tension and regulate elasticity of these pericentromeric loops [110]. Analogously, Rec8 may distribute tension along or within the loop-axis

structure of meiotic chromosomes as they are pulled by actin-driven motors, or even subjected to thermal motion (Figure S4). In the absence of Rec8, transduction of actin-mediated forces along chromosome segments would be diminished, as would their spring-like properties required for promoting allelic and taking apart ectopic interactions. Indeed, *rec8Δ* mutants in *S. pombe* exhibit defects in both chromosome compaction and pairing [111,112]. Our observation that addition of Lat B increases nonspecific interactions in *rec8Δ*, and even more so in a *rec8Δ ndj1Δ* double mutant, suggests independent contributions of actin, cohesin and telomere function in promoting and limiting chromosome interactions during meiosis.

Materials and Methods

Yeast strains

All yeast strains are isogenic derivatives of SK1 (Table S3) [113]. Parental haploid strains SBY1338 (*MAT a ho::hisG lys2 ura3Δ::hisG leu2::hisG ade2Δ::hisG trp1::hisG GAL3 flo8::LEU2-loxP-ura3 ndt80Δ::LEU2-loxP-ade2*) and SBY1448 (*MAT alpha ho::hisG lys2::GAL1-Cre-LYS2 ura3Δ::hisG leu2::hisG ade2Δ::hisG leu2::hisG ade2re-LYS2 ura3-loxP-ura3 ndt80Δ::LEU2*) were used for transformation to generate PCR-mediated knockouts [21]. Knockout mutations in SBY1338 and SBY1438 were generated by transformation using PCR-based disruption that replaced the entire open reading frame with the *kanMX4*, *natMX*, or *hphMX4* marker [114,115]. Integration of the drug-resistant markers into the appropriate genomic location and loss of wild-type markers were confirmed by PCR for every knockout strain created. The *cdc6-mn* (meiotic null) was generated by replacing the endogenous promoter of *CDC6* with the promoter of *SCC1*, which is down regulated during meiosis. The *sgs1-mn* allele was generated by placing *SGS1* under the control of the *CLB2* promoter [116]. The *rec8Δ::pREC8-SCC1* construct allows for expression of Scc1 instead of Rec8 by placing *SCC1* under the control of the Rec8 promoter [84].

Diploid strains carry an allelic pair of *loxP* sites on chromosome V (replacing *FLO8*; coordinates 377614 to 375215) and an ectopic *loxP* site on chromosome VIII (replacing *NDT80*; coordinates 356561 to 358444). Both chromosomes are ~580 kb in length with centromeres located at ~110 and ~150 kb from the right telomere, respectively. The *loxP* sites are integrated in the left arm

at sites roughly equidistant from their adjacent centromeres (*CEN5-FLO8* is ~230 kb; *CEN8-NDT80* is ~250 kb) and their adjacent telomeres (~200 kb for both intervals). In both cases, the sites are located in a region of the genome that is unremarkable for DSB distribution [85,87].

Meiotic time courses and media

Media preparation and meiotic cell culture synchronization was performed as previously described [117]. Galactose was added to final concentration of 0.03% at one hour after transfer to sporulation media (SPM) to induce expression of Cre-recombinase. At $t = 2$ hrs. after transfer to SPM, cells were either treated with 0.1% DMSO or 30 μ M Latrunculin B dissolved in DMSO.

Quantitative PCR analysis

Genomic DNA for qPCR standard curves was isolated from haploids SBY 2576 (*ho::hisG lys2-pGALI-Cre-LYS2 ura3Δ::hisG leu2::hisG ade2Δ::hisG trp1::hisG GAL3 flo8::LEU2-pGPD1-ura3*) for the allelic Cre/*LoxP* recombinant and SBY 2575 (*ho::hisG lys2-pGALI-Cre-LYS2 ura3Δ::hisG leu2::hisG ade2Δ::hisG trp1::hisG GAL3 flo8::LEU2-pGPD1-loxP-ade2*) for the ectopic Cre/*loxP* recombinant. Cells were harvested 10 hours after transfer to SPM ($t = 10$ hrs.) for DNA extraction (unless otherwise noted). DNA purification was performed by vortexing cells in the presence of 0.5 mm zirconia/silica beads (BioSpec Products, Inc.) and phenol/chloroform, followed by ethanol precipitation of the DNA. DNA from haploid strains containing only the recombinant was serially diluted to make standard curves for the corresponding primer set and *ACT1*. The following are the sequence of the primer used:

Allelic and Ectopic Forward primer: 5'-CCAAGAACT-TAGTTTCGACGGATC-3'

Allelic Reverse primer: 5'-TCGACATGATT-TATCTTCGTTTCC-3'

Ectopic Reverse primer: 5'-CAATTGTCCCCCTCCTAATA-TACCA-3'

ACT1 Forward primer: 5-AATGCAAACCGCTGCTCAAT-3'
ACT1 Reverse primer: 5'-CAAAGCTTCTGGGGCTCTGA-3'

Primers for *ACT1* reaction are used at 100 nM concentration. Primers for detection of the ectopic recombinant are used at 500 nM concentration. For detection of the allelic recombinant, the forward primer was used at 500 nM and the reverse primer was used at 900 nM. Quantitative PCR was performed on the ABI 7300 using SYBR Green Power master mix (ABI). The cycling conditions are as follows: 95° for 10 min. Followed by 40 cycles of 95° 15 sec and 60° 1 min. Collisions in all strains except for strains containing the *cdc-6mm* mutation were calculated as 4 times the recombinant copy number divided by the copy number of *ACT1* to yield number of recombinants per four chromatids. Due to the absence of meiotic replication in *cdc-6mm* mutants, collisions in *cdc-6mm* mutants were calculated as 2 times the recombinant copy number divided by the copy number of *ACT1* to yield number of recombinants for the two chromatids of the unreplicated homolog pair.

Visual homolog pairing assay

Cells were synchronized and Lat B was added as described above except that galactose was not added to the cultures. Cells were removed (250 μ l) every hour, fixed in 4% paraformaldehyde (PFA) in phosphate buffered saline (PBS; pH 7.4) for 8 minutes at room temperature. Cells were then washed once with PBS and stored at 4°C until they could be analyzed. Cell morphology and pairing levels were the same in unfixed and in fixed cells for up to

one week (data not shown). A monolayer of cells on a slide was prepared according to [118] and cells were immediately imaged at 100 \times magnification using a hybrid spinning disk confocal microscope (Intelligent Imaging Innovations) with a 488 nm laser for 150 msec exposure time per slice. Pairing was assessed visually in projected Z-stacks by determining the fraction of cells containing one GFP spot. Each Z-stack consisted of ~30 slices with 0.25 μ m separating each slice. Strains used for visualizing homolog pairing were:

SBY4503 \times SBY4504 (*MAT a/MAT alpha ho::hisG/" LEU2::tetR-GFP/" URA3::tetOx224/" his3::hisG/" ndt80Δ::NAT/"*)

SBY4506 \times SBY4507 (*MAT a/MAT alpha ho::hisG/" LEU2::tetR-GFP/" URA3::tetOx224/" his3::hisG/" ndt80Δ::NAT/" ndj1Δ::Hph/"*)

SBY4870 \times SBY4871 (*MAT a/MAT alpha ho::hisG/" LEU2::tetR-GFP/" URA3::tetOx224/" his3::hisG/" ndt80Δ::NAT/" csm4Δ::Hph/"*)

SBY4872 \times SBY4873 (*MAT a/MAT alpha ho::hisG/" LEU2::tetR-GFP/" URA3::tetOx224/" his3::hisG/" ndt80Δ::NAT/" ndj1Δ::Hph/" csm4Δ::Hph/"*).

Return to growth analysis

Cells were harvested 10 hours after transfer to SPM (unless otherwise noted). Cell aliquots were pelleted, resuspended in 2% glucose, sonicated 5 seconds at 15% maximum power using the microtip of a 550 Sonic ZD-dismembrator (Fisher Scientific), and diluted appropriately prior to plating on selective (SC-Ura) and nonselective media (YPD-Ade).

Statistical analysis

A two-tailed Student's t-test was performed for determining the *P*-value between treated and untreated cultures. All bar plots signify the mean \pm standard deviation of the mean for measured collision levels (above). The total number of independent cultures for all strains is listed in Table S2. Heatmaps indicating the *P*-values for comparison of values across multiple strains was obtained from applying a two-tailed Student's t-test followed by Sidak correction where $P = 1 - (1 - \alpha)^{1/n}$.

Supporting Information

Figure S1 Allelic collision levels in various DSB repair mutants using the RTG and qPCR assays. RTG levels. A. Both allelic and ectopic collision levels are shown for wild type and *spo11Δ* strains using qPCR and the return-to-growth (RTG) method. Sidak-corrected *P*-values incorporating these strains in the study are shown in Figure S3. B. Allelic collision levels in strains where DSB repair is altered compared to wild type. Sidak-corrected *P*-values incorporating these strains in the study are shown in Figure S3. The number of replicas is reported in Table S3. (EPS)

Figure S2 Allelic and Ectopic collision levels for all mutants. Graphical parameters are as described in Figure 3. (EPS)

Figure S3 Heatmap of allelic and ectopic collision levels for all mutants. Heatmap of Sidak adjusted *P*-values from Student's t-test comparing collision levels between relevant mutants in untreated cells. (EPS)

Figure S4 A mechanical model for homolog pairing in *ndj1Δ* and *csm4Δ* mutant backgrounds. Beginning (white panels) and ending (grey panels) snapshots of the pairing process in WT, *ndj1Δ* and *csm4Δ* mutant cells. Left pair of panels depicts untreated cells.

Right pair of panels illustrates cells treated with Lat B. See Figure 7 for description of objects.
(EPS)

Table S1 Allelic and Ectopic collision levels with and without galactose induction of *Cre*. Analysis of collision levels in WT, *spo11Δ*, *spo11Δ ndj1Δ*, *spo11Δ zip1Δ*, and *spo11Δ ndj1Δ zip1Δ* strains with and without galactose induction of *Cre* at 2 hrs post meiotic induction.
(PDF)

Table S2 Allelic and ectopic collision levels all mutants analyzed. The n values denote the total numbers of independent cultures analyzed for each strain. For most strains up to three cultures per strain per day were analyzed in parallel on the same day. WT or *spo11Δ* strains, as appropriate, were included in every experiment as a control. Strains with an n value of less than 6 were analyzed in duplicate or singly on at least two different days, respectively. To normalize collision levels per meiosis in the absence of DNA replication in *cdc6-mn* strains, collision levels are

determined as the measured recombinants per 2 chromatids, not 4 as is the case for all other reported values.
(EPS)

Table S3 Strains used for collision analysis.
(PDF)

Acknowledgments

We are grateful to JoAnne Engebrecht, Neil Hunter, Nancy Kleckner, and members of the Burgess lab, especially Daniel Elntan and Daniel Chu, for discussions. We thank Kim Nasmyth for strains carrying TetR and *telO* and Michael Dresser for sharing unpublished results.

Author Contributions

Conceived and designed the experiments: DYL CKC SMB. Performed the experiments: DYL CKC. Analyzed the data: DYL CKC SMB. Wrote the paper: DYL CKC SMB.

References

- Gerton JL, Hawley RS (2005) Homologous chromosome interactions in meiosis: diversity amidst conservation. *Nat Rev Gen* 6: 477–487.
- Tsai JH, McKee BD (2011) Homologous pairing and the role of pairing centers in meiosis. *J Cell Sci* 124: 1955–1963.
- Hunt PA, Hassold TJ (2008) Human female meiosis: What makes a good egg go bad? *Trends Genet* 24: 86–93.
- Jinks-Robertson S, Petes TD (1986) Chromosomal translocations generated by high-frequency meiotic recombination between repeated yeast genes. *Genetics* 114: 731–752.
- Goldman A, Lichten M (1996) The Efficiency of meiotic recombination between dispersed sequences in *Saccharomyces cerevisiae* depends upon their chromosomal location. *Genetics* 144: 43–55.
- Lichten M, Borts RH, Haber JE (1987) Meiotic gene conversion and crossing over between dispersed homologous sequences occurs frequently in *Saccharomyces cerevisiae*. *Genetics* 115: 233–246.
- Misteli T, Soutoglou E (2009) The emerging role of nuclear architecture in DNA repair and genome maintenance. *Nat Rev Mol Cell Biol* 10: 243–254.
- Barzel A, Kupiec M (2008) Finding a match: How do homologous sequences get together for recombination? *Nat Rev Gen* 9: 27–37.
- Mekhail K, Seebacher J, Gygi SP, Moazed D (2008) Role for perinuclear chromosome tethering in maintenance of genome stability. *Nature* 456: 667–670.
- Taddei A, Schober H, Gasser SM (2010) The budding yeast nucleus. *Cold Spring Har Perspect Biol* 2: a000612.
- Schober H, Ferreira H, Kalck V, Gehlen LR, Gasser SM (2009) Yeast telomerase and the SUN domain protein Mps3 anchor telomeres and repress subtelomeric recombination. *Genes Dev* 23: 928–938.
- Davis L, Smith GR (2006) The meiotic bouquet promotes homolog interactions and restricts ectopic recombination in *Schizosaccharomyces pombe*. *Genetics* 174: 167–177.
- Goldman ASH, Lichten M (2000) Restriction of ectopic recombination by interhomolog interactions during *Saccharomyces cerevisiae* meiosis. *Proc Natl Acad Sci U S A* 97: 9537–9542.
- Bhalla N, Dernburg AF (2008) Prelude to a division. *Ann Rev Cell and Dev Biol* 24: 397–424.
- Weiner BM, Kleckner N (1994) Chromosome pairing via multiple interstitial interactions before and during meiosis in yeast. *Cell* 77: 977–991.
- Storlazzi A, Tesse S, Gargano S, James F, Kleckner N, et al. (2003) Meiotic double-strand breaks at the interface of chromosome movement, chromosome remodeling, and reductional division. *Genes Dev* 17: 2675–2687.
- Bowring FJ, Yeadon PJ, Stainer RG, Catchside DE (2006) Chromosome pairing and meiotic recombination in *Neurospora crassa spo11* mutants. *Curr Gen* 50: 115–123.
- Loidl J, Klein F, Scherthan H (1994) Homologous pairing is reduced but not abolished in asynaptic mutants of yeast. *J Cell Biol* 125: 1191–1200.
- Baudat F, Manova K, Yuen JP, Jasim M, Keeney S (2000) Chromosome synapsis defects and sexually dimorphic meiotic progression in mice lacking *Spo11*. *Mol Cell* 6: 989–998.
- Ding DQ, Yamamoto A, Haraguchi T, Hiraoka Y (2004) Dynamics of homologous chromosome pairing during meiotic prophase in fission yeast. *Dev Cell* 6: 329–341.
- Peoples TL, Dean E, Gonzalez O, Lambourne L, Burgess SM (2002) Close, stable homolog juxtaposition during meiosis in budding yeast is dependent on meiotic recombination, occurs independently of synapsis, and is distinct from DSB-independent pairing contacts. *Genes Dev* 16: 1682–1695.
- Romanienko PJ, Camerini-Otero RD (2000) The mouse *Spo11* gene is required for meiotic chromosome synapsis. *Mol Cell* 6: 975–987.
- Pawlowski WP, Golubovskaya IN, Timofejeva L, Meeley RB, Sheridan WF, et al. (2004) Coordination of meiotic recombination, pairing, and synapsis by PHS1. *Science* 303: 89–92.
- McKim KS, Green-Marroquin BL, Sekelsky JJ, Chin G, Steinberg C, et al. (1998) Meiotic synapsis in the absence of recombination. *Science* 279: 876–878.
- Hughes SE, Gilliland WD, Cotitta JL, Takeo S, Collins KA, et al. (2009) Heterochromatic threads connect oscillating chromosomes during prometaphase I in *Drosophila* oocytes. *PLoS Genet* 5: e1000348. doi:10.1371/journal.pgen.1000348
- Dernburg AF, McDonald K, Moulder G, Barstead R, Dresser M, et al. (1998) Meiotic recombination in *C. elegans* initiates by a conserved mechanism and is dispensable for homologous chromosome synapsis. *Cell* 94: 387–398.
- MacQueen AJ, Phillips CM, Bhalla N, Weiser P, Villeneuve AM, et al. (2005) Chromosome sites play dual roles to establish homologous synapsis during meiosis in *C. elegans*. *Cell* 123: 1037–1050.
- Dernburg AF, Sedat JW, Hawley RS (1996) Direct evidence of a role for heterochromatin in meiotic chromosome segregation. *Cell* 86: 135–146.
- Kemp B, Boumil RM, Stewart MN, Dawson DS (2004) A role for centromere pairing in meiotic chromosome segregation. *Genes Dev* 18: 1946–1951.
- Hawley RS, Theurkauf WE (1993) Requirement for distributive segregation: achiasmatic segregation in *Drosophila* females. *Trends Gen* 9: 310–317.
- Stewart MN, Dawson DS (2008) Changing partners: moving from non-homologous to homologous centromere pairing in meiosis. *Trends Gen* 24: 564–573.
- Burgess SM, Kleckner N (1999) Collisions between yeast chromosomal loci *in vivo* are governed by three layers of organization. *Genes Dev* 13: 1871–1883.
- Burgess SM, Kleckner N, Weiner BM (1999) Somatic pairing of homologs in budding yeast: existence and modulation. *Genes Dev* 13: 1627–1641.
- Dekker J, Rippe K, Dekker M, Kleckner N (2002) Capturing chromosome conformation. *Science* 295: 1306–1311.
- Tsubouchi T, Roeder GS (2005) A Synaptonemal Complex Protein Promotes Homology-Independent Centromere Coupling. *Science* 308: 870–873.
- Molnar M, Kleckner N (2008) Examination of interchromosomal interactions in vegetatively growing diploid *Schizosaccharomyces pombe* cells by *Cre/loxP* site-specific recombination. *Genetics* 178: 99–112.
- Lorenz A, Fuchs J, Burger R, Loidl J (2003) Chromosome pairing does not contribute to nuclear architecture in vegetative yeast cells. *Euk Cell* 2: 856–866.
- Jin QW, Fuchs J, Loidl J (2000) Centromere clustering is a major determinant of yeast interphase nuclear organization. *J Cell Sci* 113: 1903–1912.
- Meaburn KJ, Misteli T, Soutoglou E (2007) Spatial genome organization in the formation of chromosomal translocations. *Sem Cancer Biol* 17: 80–90.
- Klein F, Mahr P, Galova M, Buonomo SB, Michaelis C, et al. (1999) A central role for cohesins in sister chromatid cohesion, formation of axial elements, and recombination during yeast meiosis. *Cell* 98: 91–103.
- Hollingsworth NM, Goetsch L, Byers B (1990) The HOP1 gene encodes a meiosis-specific component of yeast chromosomes. *Cell* 61: 73–84.
- Smith AV, Roeder GS (1997) The yeast Red1 protein localizes to the cores of meiotic chromosomes. *J Cell Biol* 136: 957–967.
- Bailis JM, Roeder GS (1998) Synaptonemal complex morphogenesis and sister-chromatid cohesion require Mek1-dependent phosphorylation of a meiotic chromosomal protein. *Genes Dev* 12: 3551–3563.
- Blat Y, Protacio RU, Hunter N, Kleckner N (2002) Physical and functional interactions among basic chromosome organizational features govern early steps of meiotic chiasma formation. *Cell* 111: 791–802.

45. Panizza S, Mendoza MA, Berlinger M, Huang L, Nicolas A, et al. (2011) Spo11-accessory proteins link double-strand break sites to the chromosome axis in early meiotic recombination. *Cell* 146: 372–383.
46. Zickler D, Kleckner N (1999) Meiotic chromosomes: integrating structure and function. *Annu Rev Genet* 33: 603–754.
47. Nag DK, Scherthan H, Rockmill B, Bhargava J, Roeder GS (1995) Heteroduplex DNA formation and homolog pairing in yeast meiotic mutants. *Genetics* 141: 75–86.
48. Latypov V, Rothenberg M, Lorenz A, Octobre G, Csutak O, et al. (2010) Roles of Hop1 and Mekl1 in meiotic chromosome pairing and recombination partner choice in *Schizosaccharomyces pombe*. *Mol Cell Biol* 30: 1570–1581.
49. Brar GA, Hochwagen A, Ec LS, Amon A (2009) The multiple roles of cohesin in meiotic chromosome morphogenesis and pairing. *Mol Biol Cell* 20: 1030–1047.
50. Carballo JA, Johnson AL, Sedgwick SG, Cha RS (2008) Phosphorylation of the axial element protein Hop1 by Mec1/Tel1 ensures meiotic interhomolog recombination. *Cell* 132: 758–770.
51. Kim KP, Weiner BM, Zhang L, Jordan A, Dekker J, et al. (2010) Sister cohesion and structural axis components mediate homolog bias of meiotic recombination. *Cell* 143: 924–937.
52. Goldfarb T, Lichten M (2010) Frequent and efficient use of the sister chromatid for DNA double-strand break repair during budding yeast meiosis. *PLoS Biol* 8: e1000520. doi:10.1371/journal.pbio.1000520
53. Trelles-Sticken E, Adelfalk C, Loidl J, Scherthan H (2005) Meiotic telomere clustering requires actin for its formation and cohesin for its resolution. *J Cell Biol* 170: 213–223.
54. Lin W, Jin H, Liu X, Hampton K, Yu HG (2011) Scc2 regulates gene expression by recruiting cohesin to the chromosome as a transcriptional activator during yeast meiosis. *Mol Biol Cell* 22: 1985–1996.
55. Cha RS, Weiner BM, Keeney S, Dekker J, Kleckner N (2000) Progression of meiotic DNA replication is modulated by interchromosomal interaction proteins, negatively by Spo11p and positively by Rec8p. *Genes Dev* 14: 493–503.
56. Bardhan A, Chuong H, Dawson DS (2010) Meiotic cohesin promotes pairing of nonhomologous centromeres in early meiotic prophase. *Mol Biol Cell* 21: 1799–1809.
57. Blat Y, Kleckner N (1999) Cohesins bind to preferential sites along yeast chromosome III, with differential regulation along arms versus the centric region. *Cell* 98: 249–259.
58. Kugou K, Fukuda T, Yamada S, Ito M, Sasanuma H, et al. (2009) Rec8 guides canonical Spo11 distribution along yeast meiotic chromosomes. *Mol Biol Cell* 20: 3064–3076.
59. Zickler D, Kleckner N (1998) The leptotene-zygotene transition of meiosis. *Annu Rev Genet* 32: 619–697.
60. Koszul R, Kleckner N (2009) Dynamic chromosome movements during meiosis: a way to eliminate unwanted connections? *Trends Cell Biol* 19: 716–724.
61. Starr DA, Fridolfsson HN (2010) Interactions between nuclei and the cytoskeleton are mediated by SUN-KASH nuclear-envelope bridges. *Annu Rev Cell Dev Biol* 26: 421–444.
62. Koszul R, Kim KP, Prentiss M, Kleckner N, Kameoka S (2008) Meiotic chromosomes move by linkage to dynamic actin cables with transduction of force through the nuclear envelope. *Cell* 133: 1188–1201.
63. Conrad MN, Lee CY, Chao G, Shinohara M, Kosaka H, et al. (2008) Rapid telomere movement in meiotic prophase is promoted by NDJ1, MPS3, and CSM4 and is modulated by recombination. *Cell* 133: 1175–1187.
64. Brown MS, Zanders S, Alani E (2011) Sustained and rapid chromosome movements are critical for chromosome pairing and meiotic progression in budding yeast. *Genetics* 188: 21–32.
65. Scherthan H, Wang H, Adelfalk C, White EJ, Cowan C, et al. (2007) Chromosome mobility during meiotic prophase in *Saccharomyces cerevisiae*. *Proc Natl Acad Sci USA* 104: 16934–16939.
66. Starr DA (2009) A nuclear-envelope bridge positions nuclei and moves chromosomes. *J Cell Sci* 122: 577–586.
67. Hiraoka Y, Dernburg AF (2009) The SUN rises on meiotic chromosome dynamics. *Dev Cell* 17: 598–605.
68. Chua PR, Roeder GS (1997) Tam1, a telomere-associated meiotic protein, functions in chromosome synapsis and crossover interference. *Genes Dev* 11: 1786–1800.
69. Conrad MN, Dominguez AM, Dresser ME (1997) Ndj1p, a meiotic telomere protein required for normal chromosome synapsis and segregation in yeast. *Science* 276: 1252–1255.
70. Trelles-Sticken E, Dresser ME, Scherthan H (2000) Meiotic Telomere Protein Ndj1p Is Required for Meiosis-specific Telomere Distribution, Bouquet Formation and Efficient Homologue Pairing. *J Cell Biol* 151: 95–106.
71. Conrad MN, Lee CY, Wilkerson JL, Dresser ME (2007) MPS3 mediates meiotic bouquet formation in *Saccharomyces cerevisiae*. *Proc Natl Acad Sci USA* 104: 8863–8868.
72. Kosaka H, Shinohara M, Shinohara A (2008) Csm4-dependent telomere movement on nuclear envelope promotes meiotic recombination. *PLoS Genet* 4: e1000196. doi:10.1371/journal.pgen.1000196
73. Wanat JJ, Kim KP, Koszul R, Zanders S, Weiner B, et al. (2008) Csm4, in collaboration with Ndj1, mediates telomere-led chromosome dynamics and recombination during yeast meiosis. *PLoS Genet* 4: e1000188. doi:10.1371/journal.pgen.1000188
74. Peoples-Holst TL, Burgess SM (2005) Multiple branches of the meiotic recombination pathway contribute independently to homolog pairing and stable juxtaposition during meiosis in budding yeast. *Genes Dev* 19: 863–874.
75. Lui DY, Peoples-Holst TL, Mell JC, Wu HY, Dean EW, et al. (2006) Analysis of close stable homolog juxtaposition during meiosis in mutants of *Saccharomyces cerevisiae*. *Genetics* 173: 1207–1222.
76. Hochwagen A, Amon A (2006) Checking your breaks: surveillance mechanisms of meiotic recombination. *Curr Biol* 16: R217–228.
77. Mell JC, Wienholz BL, Salem A, Burgess SM (2008) Sites of recombination are local determinants of meiotic homolog pairing in *Saccharomyces cerevisiae*. *Genetics* 179: 773–784.
78. Jessop L, Rockmill B, Roeder GS, Lichten M (2006) Meiotic chromosome synapsis-promoting proteins antagonize the anti-crossover activity of sgs1. *PLoS Genet* 2: e155. doi:10.1371/journal.pgen.0020155
79. Oh SD, Lao JP, Hwang PY, Taylor AF, Smith GR, et al. (2007) BLM ortholog, Sgs1, prevents aberrant crossing-over by suppressing formation of multi-chromatid joint molecules. *Cell* 130: 259–272.
80. Shinohara M, Shita-Yamaguchi E, Buerstedde JM, Shinagawa H, Ogawa H, et al. (1997) Characterization of the roles of the *Saccharomyces cerevisiae* RAD54 gene and a homologue of RAD54, RDH54/TID1, in mitosis and meiosis. *Genetics* 147: 1545–1556.
81. Klein HL (1997) RDH54, a RAD54 homologue in *Saccharomyces cerevisiae*, is required for mitotic diploid-specific recombination and repair and for meiosis. *Genetics* 147: 1533–1543.
82. Shinohara M, Gasior SL, Bishop DK, Shinohara A (2000) Tid1/Rdh54 promotes colocalization of Rad51 and Dmc1 during meiotic recombination. *Proc Natl Acad Sci USA* 97: 10814–10819.
83. Borner GV, Kleckner N, Hunter N (2004) Crossover/noncrossover differentiation, synaptonemal complex formation, and regulatory surveillance at the leptotene/zygotene transition of meiosis. *Cell* 117: 29–45.
84. Toth A, Rabitsch KP, Galova M, Schleiffer A, Buonomo SB, et al. (2000) Functional genomics identifies monopolin: a kinetochore protein required for segregation of homologs during meiosis I. *Cell* 103: 1155–1168.
85. Buhler C, Shroff R, Lichten M (2009) Genome-wide mapping of meiotic DNA double-strand breaks in *Saccharomyces cerevisiae*. *Methods Mol Biol* 557: 143–164.
86. Glynn EF, Megee PC, Yu HG, Mistrot C, Unal E, et al. (2004) Genome-wide mapping of the cohesin complex in the yeast *Saccharomyces cerevisiae*. *PLoS Biol* 2: e259. doi:10.1371/journal.pbio.0020259
87. Blitzblau HG, Bell GW, Rodriguez J, Bell SP, Hochwagen A (2007) Mapping of meiotic single-stranded DNA reveals double-stranded-break hotspots near centromeres and telomeres. *Curr Biol* 17: 2003–2012.
88. Hochwagen A, Tham WH, Brar GA, Amon A (2005) The FK506 binding protein Fpr3 counteracts protein phosphatase 1 to maintain meiotic recombination checkpoint activity. *Cell* 122: 861–873.
89. Trelles-Sticken E, Loidl J, Scherthan H (1999) Bouquet formation in budding yeast: initiation of recombination is not required for meiotic telomere clustering. *J Cell Sci* 112 (Pt 5): 651–658.
90. Spector I, Shochet NR, Blasberger D, Kashman Y (1989) Latrunculin—novel marine macrolides that disrupt microfilament organization and affect cell growth: I. Comparison with cytochalasin D. *Cell Motil Cytoskeleton* 13: 127–144.
91. Michaelis C, Ciosk R, Nasmyth K (1997) Cohesins: chromosomal proteins that prevent premature separation of sister chromatids. *Cell* 91: 35–45.
92. Ciosk R, Zachariae W, Michaelis C, Shevchenko A, Mann M, et al. (1998) An ESP1/PDS1 complex regulates loss of sister chromatid cohesion at the metaphase to anaphase transition in yeast. *Cell* 93: 1067–1076.
93. Rabitsch KP, Toth A, Galova M, Schleiffer A, Schaffner G, et al. (2001) A screen for genes required for meiosis and spore formation based on whole-genome expression. *Curr Biol* 11: 1001–1009.
94. Koszul R, Kameoka S, Weiner BM (2009) Real-time imaging of meiotic chromosomes in *Saccharomyces cerevisiae*. *Methods Mol Biol* 558: 81–89.
95. Harper L, Golubovskaya I, Cande WZ (2004) A bouquet of chromosomes. *J Cell Sci* 117: 4025–4032.
96. Obeso D, Dawson DS (2010) Temporal characterization of homology-independent centromere coupling in meiotic prophase. *PLoS ONE* 5: e10336. doi:10.1371/journal.pone.0010336
97. Wynne DJ, Rog O, Carlton PM, Dernburg AF (2012) Dynein-dependent processive chromosome motions promote homologous pairing in *C. elegans* meiosis. *The Journal of cell biology* 196: 47–64.
98. Penkner A, Tang L, Novatchkova M, Ladurner M, Fridkin A, et al. (2007) The nuclear envelope protein Matefin/SUN-1 is required for homologous pairing in *C. elegans* meiosis. *Dev Cell* 12: 873–885.
99. Yamamoto A, West RR, McIntosh JR, Hiraoka Y (1999) A Cytoplasmic Dynein Heavy Chain Is Required for Oscillatory Nuclear Movement of Meiotic Prophase and Efficient Meiotic Recombination in Fission Yeast. *J Cell Biol* 145: 1233–1250.
100. Sato A, Isaac B, Phillips CM, Rillo R, Carlton PM, et al. (2009) Cytoskeletal forces span the nuclear envelope to coordinate meiotic chromosome pairing and synapsis. *Cell* 139: 907–919.

101. Wynne DJ, Rog O, Carlton PM, Dernburg AF (2012) Dynein-dependent processive chromosome motions promote homologous pairing in *C. elegans* meiosis. *J Cell Biol* 196: 47–64.
102. Sonntag Brown M, Zanders S, Alani E (2011) Sustained and rapid chromosome movements are critical for chromosome pairing and meiotic progression in budding yeast. *Genetics* 188: 21–32.
103. Lee CY, Conrad MN, Dresser ME (2012) Meiotic chromosome pairing is promoted by telomere-led chromosome movements independent of bouquet formation. *PLoS Genet* 8: e1002730. doi:10.1371/journal.pgen.1002730
104. Cremer T, Cremer M (2010) Chromosome territories. *Cold Spring Harb Perspect Biol* 2: a003889.
105. Marshall WF, Straight A, Marko JF, Swedlow J, Dernburg A, et al. (1997) Interphase chromosomes undergo constrained diffusional motion in living cells. *Curr Biol* 7: 930–939.
106. Dion V, Shimada K, Gasser SM (2010) Actin-related proteins in the nucleus: life beyond chromatin remodelers. *Curr Opin Cell Biol*.
107. Yoshida T, Shimada K, Oma Y, Kalck V, Akimura K, et al. (2010) Actin-related protein Arp6 influences H2A.Z-dependent and -independent gene expression and links ribosomal protein genes to nuclear pores. *PLoS Genet* 6: e1000910. doi:10.1371/journal.pgen.1000910
108. Visa N, Percipalle P (2010) Nuclear functions of actin. *Cold Spring Harb Perspect Biol* 2: a000620.
109. Stephens AD, Haase J, Vicci L, Taylor RM, 2nd, Bloom K (2011) Cohesin, condensin, and the intramolecular centromere loop together generate the mitotic chromatin spring. *J Cell Biol* 193: 1167–1180.
110. Bloom K, Joglekar A (2010) Towards building a chromosome segregation machine. *Nature* 463: 446–456.
111. Ding DQ, Sakurai N, Katou Y, Itoh T, Shirahige K, et al. (2006) Meiotic cohesins modulate chromosome compaction during meiotic prophase in fission yeast. *J Cell Biol* 174: 499–508.
112. Molnar M, Bahler J, Sipiczki M, Kohli J (1995) The *rec8* gene of *Schizosaccharomyces pombe* is involved in linear element formation, chromosome pairing and sister-chromatid cohesion during meiosis. *Genetics* 141: 61–73.
113. Kane SM, Roth R (1974) Carbohydrate metabolism during ascospore development in yeast. *J Bacteriol* 118: 8–14.
114. Wach A, Brachat A, Pohlmann R, Philippsen P (1994) New heterologous modules for classical or PCR-based gene disruptions in *Saccharomyces cerevisiae*. *Yeast* 10: 1793–1808.
115. Goldstein LA, McCusker HJ (1999) Three new dominant drug resistance cassettes for gene disruption in *Saccharomyces cerevisiae*. *Yeast* 15: 1541–1553.
116. Oh SD, Lao JP, Taylor AF, Smith GR, Hunter N (2008) RecQ helicase, Sgs1, and XPF family endonuclease, Mus81-Mms4, resolve aberrant joint molecules during meiotic recombination. *Mol Cell* 31: 324–336.
117. Lui D, Burgess SM (2009) Measurement of spatial proximity and accessibility of chromosomal loci in *Saccharomyces cerevisiae* using *Cre/loxP* site-specific recombination. *Methods Mol Biol* 557: 55–63.
118. Dresser ME (2009) Time-lapse fluorescence microscopy of *Saccharomyces cerevisiae* in meiosis. *Methods Mol Biol* 558: 65–79.
119. Heun P, Laroche T, Shimada K, Furrer P, Gasser SM (2001) Chromosome dynamics in the yeast interphase nucleus. *Science* 294: 2181–2186.